1-1-1997

Spatial Correlation of Flow Induced Temperature Gradients During Tissue Heating with Vascular Geometry using CT Angiography: Implications for Thermal Therapy

Michael C. Kolios
Ryerson University, mkolios@ryerson.ca

MD Sherar
University of Toronto

AE Worthington
Robarts Research Institute

DW Holdsworth
Robarts Research Institute

JW Hunt
University of Toronto

SPATIAL CORRELATION OF FLOW INDUCED TEMPERATURE GRADIENTS DURING TISSUE HEATING WITH VASCULAR GEOMETRY USING CT ANGIOGRAPHY: IMPLICATIONS FOR THERMAL THERAPY

M.C. Kolios†, M.D. Sherar†, A.E. Worthington†, D.W. Holdsworth‡ and J.W. Hunt†
†University of Toronto and the Ontario Cancer Institute 610 University Ave., Toronto, ON Canada, M5G 2M9 and ‡Imaging Research Laboratories, Robarts Research Institute, London, Ontario Canada, N6A 5K8

INTRODUCTION

Thermal models are used to predict temperature distributions of heated tissues during thermal therapy. Blood flow plays an important role in tissue heat transfer, yet there is no universally accepted mathematical formulation to model its effects during tissue heating. A better understanding of this process would improve current models of bioheat transfer. The effects of blood flow on the temperature distribution are due to convective heat transfer caused by blood motion and are classified into the effects of thermally significant vessels (vessels with diameter greater than 0.2mm-0.4mm) and the effects of the smaller vessels of the vasculature. Theoretical models predict that large vessels create flow dependent localized temperature gradients. However, there is a paucity of experimental data that examine temperature gradients near large vessels in heated tissues. Furthermore, there are no studies that spatially correlate vessel location with measured steady state and transient temperature profiles. This work examines the flow dependence of temperature profiles recorded in heated tissues near large vessels and correlates spatial fluctuations in the temperature with vascular geometry obtained by volumetric computed tomography (CT) imaging.

METHODS

An experimental system (1) was built to examine steady state and transient temperature profiles in an 80g alcohol-fixed kidney heated by a cylindrical source. Five 60μm diameter chromel-alumel thermocouples were scanned in steps of 0.1mm enclosed in 0.2mm inner diameter quartz tubing. The kidney was submerged in a water tank at room temperature, perfused by a pump and heated by a hot water needle. For the steady state experiments the needle was perfused continuously with hot water (40-60°C) while for the transient experiments a 20 second thermal pulse was delivered through the needle (60 -70°C) and the temperature rise and decay were recorded for selected regions. The temperature measurements were repeated for several kidney inflow values ranging from 0-40 ml/min. After the heating experiments were completed, an iodine based nanoparticulate contrast agent (2) was injected in the kidney and CT data were collected using a volumetric CT scanner (3). CT intensity values along lines parallel to the thermocouples were superimposed on the temperature profiles to spatially correlate temperature fluctuations and thermally significant vessel location.

RESULTS

In the steady state experiments and for no kidney flow, a bell-shaped temperature profile is expected that peaks when the thermocouple junction is closest to the source. This is seen for the two thermocouple paths labelled “no flow” in figure 1 (a) and (c). Upon kidney perfusion however, the temperature profiles exhibit features of localized cooling and heating. In figure 1(a), a localized temperature peak appears approximately 1cm away from the source (r=7mm in the figure), increasing in magnitude for the range of flows examined. This indicates transport of heat from one region to another. Superimposed on the figure are pixel intensity values derived from the CT imaging experiments. High pixel values correspond to increased concentration of the contrast agent and thus the location of large vessels. Increased intensity values correspond well with the location of the temperature peak. Furthermore, other features seem to correlate well (r= -4mm) with the increased intensity. Figure 1(b) illustrates a snapshot of the temperature profiles for the pulsed heating experiments. The profiles were recorded at t=30s (immediately after the end of the pulse) and are plotted as a function of kidney flow. The lines connecting figures 1(a) and 1(b) indicate the range of locations for which the pulsed experiments were repeated (in steps of 0.1mm). The data in the figure insert demonstrate the profiles collected from one experiment at the location indicated by the arrow. Even for the short heating pulse of 20s, blood flow has a substantial effect on the temperature profile. At the location of the measured steady state temperature peak there is a four-fold increase in the maximum temperature reached during the pulse

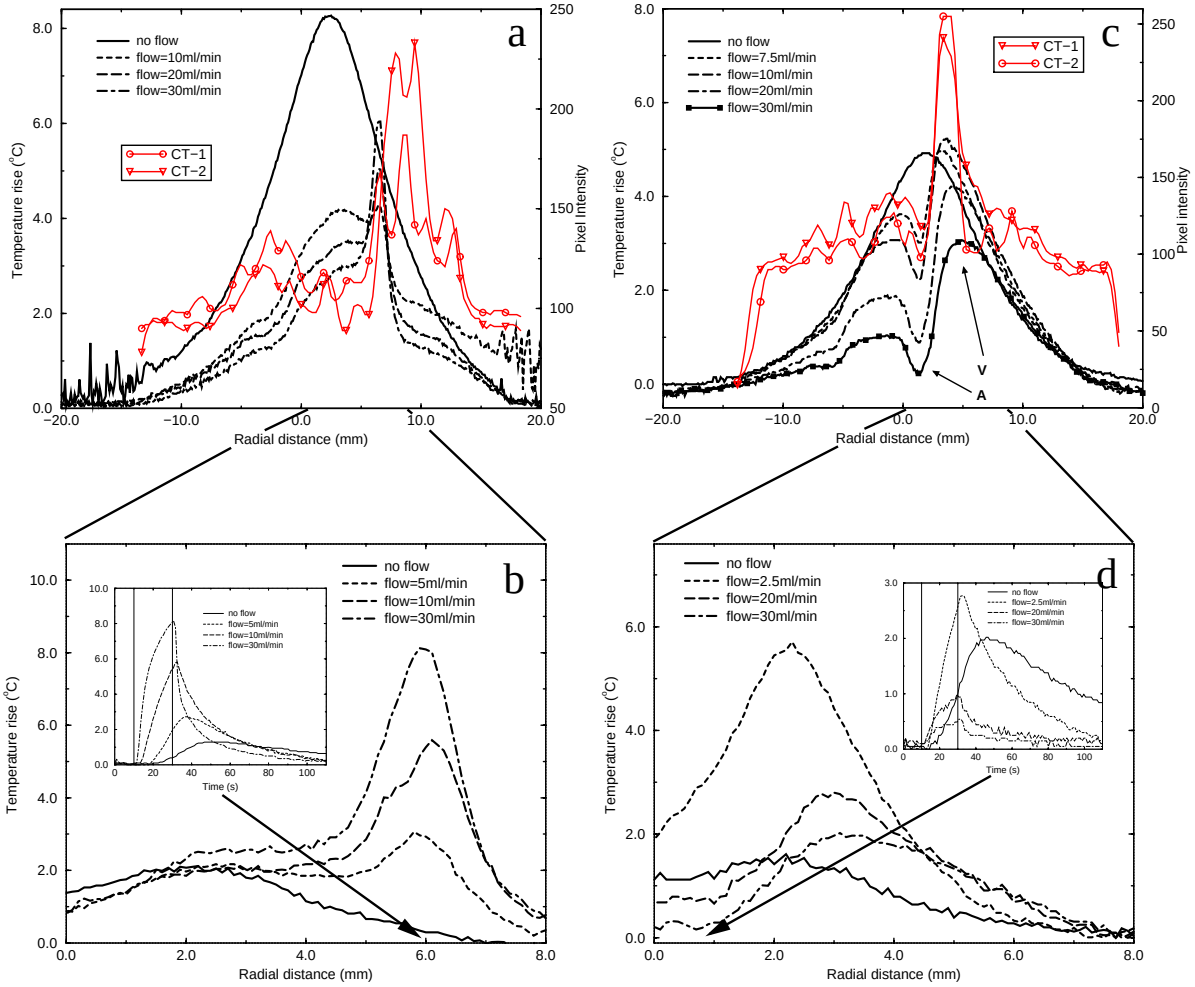

Figure 1: Steady state (a),(c) and transient (b),(d) temperature profiles measured by scanned thermocouples as a function of kidney flow. Figures (a) and (b) correspond to profiles measured by one thermocouple and (c),(d) by another. Lighter lines labelled CT-1 and CT-2 in (a) and (c) plot the pixel intensity values along lines parallel to the thermocouple tracts. Lines connecting (a) to (b) and (c) to (d) indicate the range sampled by the pulsed experiments (from +0.3 to +8.3mm in (a) and (c)). The insets in (b) and (d) show the results of individual experiments at the location indicated by the arrow.

heating and a 20s reduction in the delay time (the time delay between the initial temperature rise of the source and the temperature rise at some point r away from the source) when comparing the profiles measured for no flow and a flow of 30 ml/min. As in the steady state experiments, there is good alignment between the regions of increased CT intensity and enhanced heat transport.

Figure 1(c) and (d) represent similar data recorded by another thermocouple path located further from the source. In this case the steady state profiles indicate regions of both localized cooling and heating (labels A and V in figure 1(c)). The proximity of these regions suggest that a counter-current pair of vessels is causing the distortions. While the CT data do demonstrate increased pixel intensity in this region, only one vascular structure can be resolved. Figure 1(d) represents the temperature profiles at t= 30s for the transient experiments. As for the previous thermocouple data, perfusing the kidney significantly alters the temperature profiles even for the short heating time of 20s. Delay times are reduced and peak temperatures either increase or decrease in a flow dependent manner. Interestingly, for lows flows excess heating dominates the profile (in comparison to the no flow data) while for higher flows there is both heating and cooling. The peak and valley formed are separated by $\sim$ 2mm.

DISCUSSION

This study has examined the flow dependence of steady state and transient temperature profiles in perfused, heated tissues and has focussed on large vessels effects. The use of the kidney model allowed repeated experiments using the same flow phantom and the same thermocouple configuration. This enabled the comparison of features detected in steady state profiles with those detected in transient experiments at the same locations. Furthermore, the phantom was used for imaging experiments to detect large vessels using a volumetric CT scanner. The high spatial resolution thermocouple scanning allowed the detection of features that would not be detectable using either single point measurements or scanning in steps greater than or equal to 1mm.

The data demonstrate that to accurately predict the resulting temperature distribution in thermal treatments on must account for the effects of blood flow. Thermal models that do not account for blood flow would predict the temperature profiles labeled as "no-flow" in figure 1 which clearly are not representative of the profiles measured with flow. Hence it cannot be assumed during thermal therapy that the temperature distribution would resemble the power deposition pattern of the source. This is apparent in figure 1(b). Volumetric rendering of the CT data (data not shown) illustrated a vessel that passed by the source and the thermocouple path. The increased temperature is thought to be the result of heat transport due to the close proximity of the vessel to the source. Similar high temperatures (and thus cytotoxicity) in thermal treatments may be crucial to predict when critical structures are to be spared (*e.g.* in the brain). Furthermore, as figure 1(c) demonstrates, regions of excess localized cooling due to blood vessels may lead to decreased thermal cytotoxicity and thus treatment failure. There was good agreement when comparing the spatial location of the flow induced temperature fluctuations with increased values of CT pixel intensity thus implying that thermally significant vessels caused these fluctuations. The pulse duration in the transient experiments was 20s. It has been postulated (4) that rapid treatments may overcome the effects of blood flow on temperature distributions: it is apparent however that the heat transport properties of large vessels still plays an important role for short exposure times in these experiments.

CONCLUSIONS

Thermally significant vessels created flow dependent temperature gradients of up to 6°C/mm in the steady state experiments. The thermal response to a 20s pulse of heat demonstrated the transport properties of the vessels and that even for short exposure times large vessels can significantly alter the temperature profiles of heated tissues. Large vessels can also act as a heat source in addition to a heat sink, transporting heat from one region to another. Volumetric CT angiography confirmed the presence of thermally significant vessels at the anticipated locations and assisted in the interpretation of the temperature fluctuations observed. Future efforts in thermal modeling of heating treatments should focus on the incorporation of large vessel geometry and flow data in thermal models.

ACKNOWLEDGMENTS

The authors would like to gratefully acknowledge the financial support of the National Cancer Institute of Canada and the Ontario Cancer Treatment and Research Foundation. The first author is a recipient of a University of Toronto Open Doctoral Fellowship. The authors also acknowledge the expert help Valdemar Dabrowski and Mike Thorton of the Robarts Research Institute for performing the 3D Computed Tomography studies and Dr. Gregory McIntire of Nycomed Corporation for providing the contrast agent used in the studies and his advice. Finally, the authors thank Dalton Newcombe and the Electronics Department of the Princess Margaret Hospital for general help.

REFERENCES

[1] M. C. Kolios, M. D. Sherar, A. E. Worthington, and J. W. Hunt. Modeling temperature gradients near large vessels in perfused tissues. In M. A. Ebadian and P. H. Oosthuizen, editors, *Fundamentals of Biomedical Heat Transfer*, pages 23–30, HTD-Vol.295, 1994. American Society of Mechanical Engineers.

[2] G. S. Gazelle, G. L. Wolf, E. R. Bacon, G. L. McIntire, E. R. Cooper, and J. L. Toner. Nanocrystalline computed tomography contrast agents for blood-pool and liver-spleen imaging. *Investigative Radiology*, 29(Suppl 2):S286–8, 1994.

[3] D. W. Holdsworth, M. Drangova, and A. Fenster. A high-resolution XRII-based quantitative volume CT scanner. *Medical Physics*, 20((2 Pt 1)):449–62, 1993.

[4] B. E. Billard, K. Hynynen, and R. B Roemer. Effects of physical parameters on high temperature ultrasound hyperthermia. *Ultrasound in Medicine and Biology*, 16:409–420, 1990.